Published in final edited form as:

Science. 2019 July 05; 365(6448): 53–60. doi:10.1126/science.aau9263.

A COPII subunit acts with an autophagy receptor to target endoplasmic reticulum for degradation

Yixian Cui[1], **Smriti Parashar**[1], **Muhammad Zahoor**[2,†], **Patrick G. Needham**[3,†], **Muriel Mari**[4], **Ming Zhu**[1], **Shuliang Chen**[1], **Hsuan-Chung Ho**[1], **Fulvio Reggiori**[4], **Hesso Farhan**[2,†], **Jeffrey L. Brodsky**[3,†], **Susan Ferro-Novick**[1,*]

[1]Department of Cellular and Molecular Medicine, University of California at San Diego, La Jolla, CA 92093-0668 [2]Institute of Basic Medical Sciences, Department of Molecular Medicine, University of Oslo. Sognsvannsveien 9, 0372 Oslo, Norway [3]Department of Biological Sciences, University of Pittsburgh, Pittsburgh, PA 15260 [4]Department of Biomedical Sciences of Cells and Systems, University of Groningen Medical Center, The Netherlands

Abstract

The COPII-cargo adaptor complex, Lst1-Sec23, selectively sorts proteins into vesicles that bud from the endoplasmic reticulum (ER) and traffic to the Golgi. Improperly folded proteins are prevented from exiting the ER and are degraded. ER-phagy is an autophagic degradation pathway that utilizes ER-resident receptors. Working in yeast, we found an unexpected role for Lst1-Sec23 in ER-phagy that was independent from its function in secretion. Upregulation of the stress inducible ER-phagy receptor, Atg40, induced the association of Lst1-Sec23 with Atg40 at distinct ER domains to package ER into autophagosomes. Lst1-mediated ER-phagy played a vital role in maintaining cellular homeostasis by preventing the accumulation of an aggregation-prone protein in the ER. Lst1 function appears to be conserved because its mammalian homologue, SEC24C, was also required for ER-phagy.

One Sentence Summary

Different COPII coat subunits direct ER contents onto two distinct pathways: the secretory pathway and ER-phagy

Vesicle transport cargo adaptors sort and concentrate cargo into transport vesicles at specific stages of membrane traffic (1, 2). At the endoplasmic reticulum (ER), the Sec24 subunit of the major COPII-cargo adaptor complex, Sec24-Sec23, binds to the cytosolic domain of ER transmembrane proteins and packages them into vesicles that traffic to the Golgi (1). Yeast

*Correspondence should be addressed to: Dr. Susan Ferro-Novick, Department of Cellular and Molecular Medicine, University of California at San Diego, George Palade Labs, room 315, Phone: (858) 246-0466, Fax: (858) 534-7688, sfnovick@ucsd.edu.
†equal contribution

Author contributions: Y.C., S.P., M.Z., P.G.N., M.M., M.Z., S.C., H.-C.H., F.R., H.F., J.L.B. and S.F.-N. designed research and analyzed data; Y.C., S.P., M.Z., P.G.N., M.M., M.Z., S.C. and H.-C.H., performed research; and S.F.-N., J.L.B., F.R., Y.C., S.P., M.M. and H.F. wrote the paper.

Competing interests: Authors declare no competing interests.

Data and materials availability: All data are available in the main text or the supplementary materials.

also has two Sec24 paralogs, Iss1/Sfb2 (56% identity) and Lst1/Sfb3 (23% identity), which form secretory cargo adaptor complexes with Sec23. Mammals have four SEC24 isoforms. The mammalian SEC24 homologues (SEC24A and SEC24B) are 50% identical, but only share 20% identity with the Lst1 homologues (SEC24C and SEC24D) that are also 50% identical to each other (3).

ER homeostasis is maintained by the unfolded protein response (UPR), which is upregulated by ER stressors, such as the accumulation of unfolded or misfolded proteins in the ER. The UPR restores homeostasis by a variety of mechanisms, including the activation of signaling pathways that increase the production of the chaperones and enzymes that promote and regulate protein folding (4). To prevent improperly folded proteins from entering the secretory pathway, ER-associated degradation (ERAD) recognizes terminally misfolded proteins and retrotranslocates them into the cytosol for degradation by the proteasome (5). ERAD, however, is unable to clear all aberrant proteins from the ER (6). Macroautophagy (herein called autophagy) of the ER, or ER-phagy, could be part of a global ER stress response that restores cellular homeostasis when ERAD and/or the UPR fail to respond. There are two major types of autophagy pathways, bulk and selective (7). During starvation, bulk autophagy uses autophagosomes to scavenge cytoplasmic components for nutrients. To rapidly increase autophagosome number, COPII vesicles are rerouted to serve as a membrane source for bulk autophagy (7, 8). Selective pathways, instead, employ autophagy receptors to package cargo into autophagosomes. These cargoes include damaged or superfluous organelles, protein aggregates and pathogens (9).

Although ER-phagy was initially described in 2005 (10), it was not until the first ER-phagy receptors were identified that the process was thought to be selective (11, 12). ER-phagy occurs at discrete foci on the ER (13), however, the autophagy receptors that load ER into autophagosomes are dispersed throughout the contiguous network of the ER. How sites on the ER are targeted for ER-phagy is unclear. We reasoned that cytosolic machinery that recognizes and binds to ER-phagy receptors may play a role in marking specific sites on the ER where autophagy will occur. Because COPII coat subunits are known to participate in membrane budding events at the ER (1), we asked if coat subunits play a role in sequestering ER domains into autophagosomes during ER-phagy.

Lst1 is required for ER-phagy, but not bulk autophagy

ER-phagy is typically induced in yeast by treating cells for 12-24 h with rapamycin, a TOR kinase inhibitor that mimics nutrient starvation (10, 11). Rapamycin also upregulates the expression of the ER-phagy receptor, Atg40, which increases ER-phagy activity (10, 11). Atg40, a reticulon-like ER membrane protein, is required for cortical and cytoplasmic ER degradation, and also contributes to nuclear ER degradation. Nuclear ER turnover is predominantly facilitated by Atg39, a nucleophagy receptor (11).

We initiated our studies by asking if COPII coat subunits play a role in ER-phagy. The long incubation period with rapamycin to induce ER-phagy precluded us from analyzing temperature-sensitive mutants harboring COPII mutations because they die quickly at their restrictive temperature. The *lst1Δ*, *iss1Δ* and *sec24-3A* mutants, however, do not

significantly impair growth or secretion (14, 15). In *sec24-3A* cells, bulk autophagy is defective as a consequence of a failure to phosphorylate Sec24 at T324, T325, and T328 (15). Sec24 phosphorylation at these sites, which are conserved in Iss1, enables COPII coated vesicles to bind the core autophagy machinery (15). We found a defect in the degradation of the ER protein Sec61 in *lst1Δ*, but not in the *sec24-3A iss1Δ* and *iss1Δ* mutants (Fig. 1A-D; Fig. S1A-C). One of the kinases that phosphorylates Sec24 during bulk autophagy, Hrr25 (15), was also dispensable for ER-phagy (Fig. S1D-E). Furthermore, Sec24 phosphorylation was not needed for pexophagy (Fig. S2A-B) and mitophagy (Fig. S2D-E). The degradation of Rtn1, which marks ER tubules, the edges of sheets and the nuclear ER in a small fraction of cells (16), was also defective in the *lst1Δ* mutant (Fig. 1E-F; Fig. S3A-B). Similarly, a third ER protein, Per33, was degraded less efficiently in *lst1Δ* cells (Fig. S3C-F). Like Sec61, Per33 resides on the nuclear, cortical, and cytoplasmic ER (17). In addition to rapamycin, Lst1-mediated ER degradation was also induced by growth to stationary phase (Fig. S4A-C).

To ask if Lst1 functions in bulk autophagy, we measured the activation of vacuolar alkaline phosphatase (Pho8Δ60) after starvation (Fig. S4D), as well as the cleavage of GFP-Atg8 in the vacuole (Fig. S4E-F) 24 h after rapamycin treatment (18). When bulk autophagy is induced, GFP-Atg8 and Pho8Δ60 are delivered to the vacuole, where Pho8Δ60 is activated by proteolytic cleavage. No defect in bulk autophagy was detected in *lst1Δ* cells by either assay. Additionally, Lst1 was not needed for pexophagy (Fig. S2B-C), mitophagy (Fig. S2E-F), or the biosynthetic cytosol to vacuole targeting (Cvt) pathway (Fig. S2G), which also uses autophagy machinery (18). Thus, Lst1 and its paralogue Sec24, appeared to function in different autophagy pathways. While phosphorylation of the Sec24 membrane distal surface is required for bulk autophagy (15), it was dispensable for ER-phagy. In contrast, Lst1 acted exclusively in ER-phagy.

Lst1 is primarily known for the formation of larger COPII coated vesicles and the trafficking of GPI anchored proteins (1). Unlike Sec24, Lst1 cannot package the ER-Golgi fusion machinery (SNAREs) into COPII vesicles. Consequently, vesicles containing Lst1, but not Sec24, are unable to fuse with the Golgi (19). When we measured ER-phagy in two *lst1* mutants (*LST1*-B1 and *LST1*-B2) that disrupt the packaging of GPI anchored proteins into COPII vesicles (20), no ER-phagy defect was observed (Fig. S5A-D). Thus, the role of Lst1 on the secretory pathway can be uncoupled from its contribution to ER-phagy. These results establish an unanticipated role for this conserved coat protein in autophagy.

Lst1 acts in concert with Atg40

Sec61-GFP positive ER cisternae and foci accumulated in rapamycin-treated *atg40Δ* and *lst1Δ* mutants (Fig. S6A-B). Furthermore, the ER degradation defect in the *lst1Δatg40Δ* double mutant was not significantly different than either single knockout (Fig. S6C-F). These findings implied that Lst1 and Atg40 function in the same pathway. Because elevated levels of autophagy receptors increase ER-phagy and ER-containing autophagosome number (11, 12), ER-phagy receptors are thought to play a role in packaging ER into autophagosomes (12). To address if Lst1 works with Atg40 to perform this function, we induced Atg40 expression with rapamycin (11) and asked if this promotes an association

with Lst1. To assess the colocalization of Lst1-3xGFP with Atg40-2xmCherry, we focused on non-cortical Atg40 puncta because previous studies indicated these more central puncta have greater accessibility to the autophagy machinery (17). Sec24-GFP and Sec13-GFP, a component of the COPII coat scaffold complex (Sec13-Sec31) (1), were examined as controls. Although all COPII coat subunits mark ER exit sites (ERES) in nutrient-rich growth conditions (21), only Lst1-3xGFP and its partner Sec23-GFP showed increased colocalization with Atg40-2xmCherry puncta (Fig. 2A-C; Fig. S7A-C). Unlike Atg40, Lst1 and Sec23 expression did not increase with rapamycin treatment (Fig. S7D). The number of Lst1-3xGFP and Sec23-GFP puncta was also unchanged (Fig. S7E). While previous studies showed *CUP1*-driven Atg40 overexpression only increased ER-phagy in the presence of rapamycin (11), overexpression was sufficient to drive Atg40 colocalization with Lst1 (Fig. S8A-B). Rapamycin also induced the expression of the nucleophagy receptor, Atg39 (11), but did not induce the colocalization of Lst1 with Atg39 (Fig. S8C-D). Furthermore, Lst1 did not contribute to the degradation of the nuclear ER marker Hmg1 (Fig. S8E-H).

Selective autophagy receptors bind to the ubiquitin-like protein, Atg8, at sites of autophagosome formation (9). Consistent with the proposal that Lst1 functions with Atg40 to target ER domains for degradation, rapamycin induced Atg8-Lst1 colocalization in wild-type (WT), but not *atg40Δ* cells (Fig. 2D; Fig. S9A). In contrast, Atg8 showed increased colocalization with two COPII coat subunits required for bulk autophagy, Sec24 and Sec13 (22), in both WT and *atg40Δ* cells (Fig. 2D; Fig. S9A). Because Sec23 is a binding partner for both Lst1 and Sec24, the colocalization of Atg8 with Sec23 was only partially dependent on Atg40 (Fig. 2D; Fig. S9A).

Next, we asked whether ER organization is important for the colocalization of Lst1 with Atg40. Lnpl is an ER protein that resides at and stabilizes the three-way junctions that form when two tubules fuse to each other (23). In its absence, ER network rearrangements are disrupted and Atg40 puncta fail to access the autophagy machinery (17). As a consequence, ER is not packaged into autophagosomes in *lnp1Δ* cells (17). We found that Lst1-3xGFP failed to colocalize with Atg40-2xmCherry (Fig. 2E, Fig. S9B; also see Pearson's coefficient in Fig. S9C) in *lnp1Δ* cells. Furthermore, even though Lst1-3xGFP and RFP-Atg8 puncta appeared unaltered in the *lnp1Δ* mutant, Atg8 also failed to colocalize with Lst1 (Fig. 2F; Fig. S9D). We propose that Atg8-Lst1 colocalizing puncta (usually one per cell) represent active ER-phagy sites stabilized by Lnp1. Although Atg40 puncta tend to accumulate at the cell periphery in Lnp1-depleted cells (17), the distribution of Atg40 puncta was unperturbed in *lst1Δ* cells (Fig. S9E).

The localization studies described above suggested that Lst1 and Atg40 interact with each other during ER-phagy. Lst1 could interact with Atg40 via its cytosolic domain (11), however, this possibility could not be tested because the cytoplasmic domain was unstable. We were also unable to express full length Atg40 in bacteria. Instead, to address whether Lst1 interacts with Atg40, binding studies were performed with lysates prepared from untreated and rapamycin-treated cells expressing Atg40-3xFLAG. Atg40-3xFLAG from both lysates bound to purified bacterially produced GST-Lst1, but not GST-Sec13, GST-Sec24 (Fig. 3A; Fig. S10A and Fig. S10C), or GST-Sec23 (Fig. S10B). GST-Lst1 also failed to bind to two other ER proteins, Ufe1 and Yip1 (Fig. S10D). These findings indicate that

Lst1, but not Sec24 or other COPII coat subunits, binds to Atg40. Sec13-Sec31 could have failed to associate with Atg40 because the binding of Lst1-Sec23 to Atg40 sterically hindered its interaction. Supporting the proposal that the interaction of Atg40 with Lst1 is needed for ER-phagy, the rapamycin-induced degradation of Lst1-GFP required Atg40, and Atg40-GFP degradation required Lst1 (Fig. S11A-H).

To count ER-containing autophagosome numbers in the *lst1Δ* mutant, cells depleted of the vacuolar protease Pep4 were examined by conventional electron microscopy (EM) (Fig. 3B-D). While autophagic bodies were absent in the *atg14Δ* mutant, which blocks autophagosome formation (Fig. 3B-D), the number of autophagosomes formed in the *lst1Δ* mutant was the same as in WT (Fig. 3D). In contrast, a significant reduction in autophagic bodies that contained ER was observed in the *lst1Δ* mutant (Fig. 3B-C). Consistent with the proposal that Lst1 works with Atg40 to package cortical and cytoplasmic ER into autophagosomes, the *lst1Δ* defect was comparable to that seen in *atg40Δ* cells (Fig. 3B-C).

ER stress upregulates Atg40

In mammalian cells, the putative ER-phagy receptor, FAM134B, targets ERAD-insensitive substrates to autophagy (6). How the ER communicates with the autophagy machinery when ERAD does not respond or is overwhelmed is unknown.

The Z variant of human alpha-1 antitrypsin (ATZ) is an aggregation-prone ERAD substrate that is also targeted to the lysosome via non-autophagosome-mediated (24) and autophagosome-mediated pathways (25, 26). When ATZ is highly overexpressed in yeast under the inducible galactose promoter (*GAL1*), excess ATZ not degraded by ERAD is directed to the vacuole via two pathways, vacuolar protein sorting and autophagy (27). Blocking the latter pathway leads to the accumulation of ATZ aggregates in the ER (27). Currently it is unknown if this autophagosome-mediated pathway is ER-phagy. To ask whether ATZ aggregates in the absence of Atg40 or Lst1, microsomal membrane fractions prepared from WT, *atg14Δ, atg40Δ* and *lst1Δ* cells were analyzed on sucrose gradients. Soluble ATZ was primarily found at the top of the WT gradient, while ATZ from mutant lysates was largely in the pellet (Fig. 4A-C; Fig. S12A-B). Aggregation appeared to result from a block in ER-phagy, because significantly less ATZ was observed in the pellet when lysates from the *lst1*-B1 mutant were examined (Fig. S12C). The *lst1*-B1 mutant disrupts membrane traffic (20), but not ER-phagy (Fig. S5). Aggregation was also specific to misfolded ATZ, because appreciably less wild-type M variant alpha-1 antitrypsin (ATM) was observed in the pellet when lysates from *lst1Δ* or *atg40Δ* cells were examined (Fig. 4D). Consistent with this observation, a portion of the ATM, but not ATZ, was secreted (Fig. S12D). Thus, only mutant alpha-1 antitrypsin aggregated in the ER in the absence of ER-phagy. It is of note that in the pancreas the loss of the ER-phagy receptor, CCPG1, leads to the accumulation of aggregated proteins in the ER (13).

Previous studies showed that multiple COPII coat subunits, including Sec24 and Lst1, are targets of the UPR (28). To ask if Atg40 is also a UPR target, we overexpressed ATZ in the presence or the absence of Ire1, an ER transmembrane kinase. Ire1 triggers the UPR (29). ATZ induction enhanced Atg40 expression in WT cells (Fig. 5A-B, compare with Fig.

S12E). Furthermore, Atg40 expression and ATZ accumulation were further enhanced in *ire1Δ* mutant cells, which block the UPR and augment ER stress (4, 29) (Fig. 5A-B). In contrast, overexpressed ATM did not increase Atg40 expression in the *ire1Δ* mutant (Fig. S12F). To determine whether the loss of Atg40 induces the UPR, we examined pathway induction by flow cytometry in cells carrying an integrated UPR-regulated GFP reporter. While the *atg39Δ* (Fig. 5C), and *sec24-3A iss1Δ* mutants behaved like WT (Fig. S12G), the level of UPR induction in the *atg40Δ* and *lst1Δ* mutants was the same as in an ERAD-deficient *hrd1Δ* strain (Fig. 5C) (5). Thus, although Atg40 was not found to be a UPR target, the UPR responded to the loss of ER-phagy.

Because Atg40 expression is not under the control of the UPR, we next sought to identify the pathway that regulates it. ER stress is known to modulate the expression of core autophagy machinery (30). Therefore, we considered the possibility that autophagy transcriptional regulators control Atg40 expression. Pho23, which associates with the histone deacetylase large complex (Rpd3L), is a transcriptional repressor of autophagy that modulates autophagosome abundance via Atg9 (31). We found that, Atg40, but not the UPR targets, Kar2 and Lst1, were upregulated in the *rpd3Δ* and *pho23Δ* strains (Fig. 5D-E). Atg40 and Atg9 mRNA levels also increased in these mutants (Fig. 5F), indicating that the Atg40 ER-phagy receptor is a target of the same transcriptional regulators that modulate Atg9 and other core autophagy machinery.

Mammalian SEC24C is required for ER-phagy

It was recently reported that SEC24A and SEC24B, but not SEC24C and SEC24D, contribute to bulk autophagy (32). To ask if any of the SEC24 isoforms are required for ER-phagy in mammalian cells, each of the four isoforms were knocked-down by siRNA in U2OS cells (Fig. S13A). We then monitored the delivery of two ER-phagy receptors, FAM134B and RTN3, to lysosomes in the Torin2 (TOR inhibitor2) treated SEC24-depleted cells. We chose to examine these two mammalian ER-phagy receptors because Atg40 has a domain structure that is similar to FAM134B, yet localizes to the tubular ER like RTN3 (12, 33). 3xFLAG-FAM134B was resistant to degradation in SEC24C-depleted cells, but sensitive in cells depleted of SEC24A, SEC24B or SEC24D (Fig. 6A; Fig. S13B). Moreover, the delivery of 3xFLAG-FAM134B to lysosomes (LAMP1) required SEC24C and ULK1, a component of the autophagosome biogenesis machinery (Fig. 6B-C; Fig. S13C). The delivery of RTN3 to lysosomes was also SEC24C and ULK1-dependent (Fig. 6D-E; Fig. S14). Thus, in mammals, as in yeast, TOR inhibition stimulated the delivery of ER to lysosomes via Lst1/SEC24C-mediated ER-phagy.

Discussion

Here we report a noncanonical role for the COPII-cargo adaptor complex, Lst1-Sec23, and show that it functions with the ER-phagy receptor, Atg40, to specify ER domains for ER-phagy. By analogy to its role as a cargo adaptor in vesicle traffic (20), Lst1-Sec23 may sort ER domains into autophagosomes via an interaction with the cytoplasmic domain of Atg40 (Fig. SI5). Several lines of evidence highlight the key events mediated by Lst1 on this pathway. First, when Atg40 expression was upregulated by the TOR inhibitor rapamycin, the

Lst1-Sec23 complex associated with Atg40 puncta. Second, in accord with the proposal that the colocalization of Lst1 with Atg40 is needed for ER-phagy, Lst1 failed to colocalize with Atg40 and Atg8 in the *lnp1Δ* mutant. Lnp1 is needed for ER organization and the incorporation of ER into autophagosomes (17). Third, consistent with a role in ER packaging, Lst1 was required for the degradation of Atg40, and the number of ER-containing autophagosomes was significantly reduced in the *lst1Δ* mutant.

To date, six ER-phagy receptors have been identified in mammalian cells (12, 13, 33-37). While some receptors respond to starvation, others only respond to ER stress, and some respond to both. Here we have shown that Atg40 responds to starvation and ER stress. It was upregulated by both rapamycin (11), and the overexpression of an aggregation-prone misfolded secretory protein (ATZ). In the latter case, the induction of Lst1-mediated ER-phagy reduced the level of aggregated ATZ in the ER (Fig. S15). Consistent with the observation that a TOR inhibitor upregulates Atg40 (11), we found that Atg40 expression is modulated by autophagy transcriptional regulators. Recent studies have shown that ER stress inhibits TOR (38). Thus, TOR-dependent autophagy transcriptional regulators may also modulate the upregulation of ER-phagy receptors for the purpose of reducing ER protein aggregation.

Our findings imply that a specific subcomplex of the COPII coat, that contains Lst1-Sec23, binds to Atg40 to package ER domains into autophagosomes during ER-phagy (Fig. S15). ER-phagy occurs at distinct sites on the ER that we have named **ERPHS** (**ER**-**ph**agy **s**ites). The absence of Sec24 from these sites distinguishes them from the Sec24 containing **ERES** (**ER e**xit **s**ites) that bud conventional COPII vesicles (Fig. S15). Because previous studies in yeast did not reveal a significant accumulation of cytosolic ER fragments during ER-phagy, it was suggested that ER domains are engulfed into autophagosomes on the ER network, or in close proximity to the network (10) (Fig. S15). We found Lst1-GFP was degraded in the vacuole in an Atg40-dependent fashion (Fig. S15), indicating that ER fragments were packaged into autophagosomes before they completely uncoated. Because the Lst1-Sec23 complex cannot package SNAREs, fragments that bud from the ER cannot fuse with the Golgi prior to their incorporation into autophagosomes.

The formation of **ERPHS** in yeast was dependent on the ER protein Lnp1, which is needed for stable three-way ER junctions (Fig. S15) (23). Consistent with this observation, the mammalian ER-phagy receptor, TEX264, concentrates and colocalizes with LC3 (Atg8 homologue in mammals) at ER junctions (36, 37). The localization of LNP1 to ER junctions depends on ATLASTIN, which is also required for ER-phagy (16, 39, 40). Furthermore, ATLASTIN 3 (ATL3) has recently been reported to be an ER-phagy receptor (35). Mutations in ATLASTIN and LNP1 are associated with hereditary spastic paraplegias (HSP) and HSP-like neuropathies (41, 42). The ER-phagy receptor FAM134B, which is needed for both ER-phagy and autophagosome-independent ER-to-lysosome degradation (12, 24), is linked to sensory neuron function (12).

The mammalian Lst1 homologue, SEC24C, was also required for the delivery of ER sheets (FAM134B) and tubules (RTN3) to lysosomes for degradation. This observation is in accord with recent data showing that the interactome for the ER-phagy receptor, RTN3, includes

SEC24C but not the other SEC24 isoforms (33). Although professional secretory cells are insensitive to SEC24C depletion, its loss in postmitotic neurons leads to microcephaly and perinatal death (43). While SEC24C and SEC24D are ~50% identical, their functions only partially overlap in the brain (43), and we did not detect a significant role for SEC24D in ER-phagy. Because our experiments and the RTN3 interactome analysis both used U2OS cells, it remains formally possible that other cell types may require SEC24D for ER-phagy. Together, these findings suggest that ER-phagy plays a crucial role in maintaining neuronal homeostasis.

In summary, we propose that in yeast and mammals, COPII cargo adaptors package different cargoes (secretory proteins or ER domains) into membranes and target theses cargoes to distinct pathways. Our findings imply that **ERES**, which bud canonical COPII vesicles that traffic on the secretory pathway, are distinct from the **ERPHS** used in autophagy. The secretory and ER-phagy pathways also appear to be regulated by different stress response pathways. Secretory protein homeostasis is regulated by the UPR, while ER-phagy depends on TOR-dependent autophagy transcriptional regulators.

Supplementary Material

Refer to Web version on PubMed Central for supplementary material.

Acknowledgments

We thank Shuaipeng Ma for technical assistance during the early phase of these studies, Randy Hampton for the 4xUPRE-GFP plasmid and the use of his flow cytometer, Elizabeth Miller for plasmids, and Andrea Lougheed for assistance in the preparation of figures. We also thank the UCSD School of Medicine microscopy core for use of their Volocity software.

Funding: Salary support for S.F-N., Y.C., S.P., M.Z., S.C. and H.-C.H. was provided by the ALPHA-1 FOUNDATION and NIGMS under award numbers R01GM114111, R01GM115422 and R35GM131681. Salary support for P.G.N. and J.L.B was provided by grants P30DK79307, 1R01GM75061 and R35GM131732. H.F. is supported by the Norwegian Research Council, the Norwegian Cancer Society, and the Ander Jahre Foundation. F.R. is supported by Marie Skłodowska-Curie Cofund (713660), Marie Skłodowska-Curie ITN (765912), ALW Open Program (ALWOP.310), ZonMW VICI (016.130.606) and ZonMW TOP (91217002) grants. M.M. is supported by an ALW Open Program grant (ALWOP.355).

References

1. Gomez-Navarro N, Miller E, Protein sorting at the ER-Golgi interface. J Cell Biol 215, 769–778 (2016). [PubMed: 27903609]
2. Kirchhausen T, Bonifacino JS, Riezman H, Linking cargo to vesicle formation: receptor tail interactions with coat proteins. Curr Opin Cell Biol 9, 488–495 (1997) [PubMed: 9261055]
3. Tang BL, Kausalya J, Low DY, Lock ML, Hong W, A family of mammalian proteins homologous to yeast Sec24p. Biochem Biophys Res Commun 258, 679–684 (1999). [PubMed: 10329445]
4. Walter P, Ron D, The unfolded protein response: from stress pathway to homeostatic regulation. Science 334, 1081–1086 (2011). [PubMed: 22116877]
5. Brodsky JL, Cleaning up: ER-associated degradation to the rescue. Cell 151, 1163–1167 (2012). [PubMed: 23217703]
6. Forrester A et al., A selective ER-phagy exerts procollagen quality control via a Calnexin-FAM134B complex. EMBO J 38, (2019).
7. Davis S, Wang J, Ferro-Novick S, Crosstalk between the Secretory and Autophagy Pathways Regulates Autophagosome Formation. Dev Cell 41, 23–32 (2017). [PubMed: 28399396]

8. Shima T, Kirisako H, Nakatogawa H, COPII vesicles contribute to autophagosomal membranes. J Cell Biol, 218, 1503–1510 (2019). [PubMed: 30787039]

9. Anding AL, Baehrecke EH, Cleaning House: Selective Autophagy of Organelles. Dev Cell 41, 10–22 (2017). [PubMed: 28399394]

10. Hamasaki M, Noda T, Baba M, Ohsumi Y, Starvation triggers the delivery of the endoplasmic reticulum to the vacuole via autophagy in yeast. Traffic 6, 56–65 (2005). [PubMed: 15569245]

11. Mochida K et al., Receptor-mediated selective autophagy degrades the endoplasmic reticulum and the nucleus. Nature 522, 359–362 (2015). [PubMed: 26040717]

12. Khaminets A et al., Regulation of endoplasmic reticulum turnover by selective autophagy. Nature 522, 354–358 (2015). [PubMed: 26040720]

13. Smith MD et al., CCPG1 Is a Non-canonical Autophagy Cargo Receptor Essential for ER-Phagy and Pancreatic ER Proteostasis. Dev Cell 44, 217–232 e211 (2018). [PubMed: 29290589]

14. Roberg KJ, Crotwell M, Espenshade P, Gimeno R, Kaiser CA, LST1 is a SEC24 homologue used for selective export of the plasma membrane ATPase from the endoplasmic reticulum. J Cell Biol 145, 659–672 (1999). [PubMed: 10330397]

15. Davis S et al., Sec24 phosphorylation regulates autophagosome abundance during nutrient deprivation. eLife 5, (2016).

16. Chen S, Novick P, Ferro-Novick S, ER network formation requires a balance of the dynamin-like GTPase Sey1p and the Lunapark family member Lnp1p. Nat. Cell Biol. 14, 707–716 (2012). [PubMed: 22729086]

17. Chen S, Cui Y, Parashar S, Novick PJ, Ferro-Novick S, ER-phagy requires Lnp1, a protein that stabilizes rearrangements of the ER network. Proc Natl Acad Sci U S A, 115, 6237–6244 (2018). [PubMed: 29848630]

18. Klionsky DJ, Cuervo AM, Seglen PO, Methods for monitoring autophagy from yeast to human. Autophagy 3, 181–206 (2007). [PubMed: 17224625]

19. Miller E, Antonny B, Hamamoto S, Schekman R, Cargo selection into COPII vesicles is driven by the Sec24p subunit. EMBO J 21, 6105–6113 (2002). [PubMed: 12426382]

20. Miller EA et al., Multiple cargo binding sites on the COPII subunit Sec24p ensure capture of diverse membrane proteins into transport vesicles. Cell 114, 497–509 (2003). [PubMed: 12941277]

21. Iwasaki H, Yorimitsu T, Sato K, Distribution of Sec24 isoforms to each ER exit site is dynamically regulated in Saccharomyces cerevisiae. FEBS Lett 589, 1234–1239 (2015). [PubMed: 25896017]

22. Hamasaki M, Noda T, Ohsumi Y, The early secretory pathway contributes to autophagy in yeast. Cell Struct Funct 28, 49–54 (2003). [PubMed: 12655150]

23. Chen S et al., Lunapark stabilizes nascent three-way junctions in the endoplasmic reticulum. Proc Natl Acad Sci U S A 112, 418–423 (2015). [PubMed: 25548161]

24. Fregno I et al., ER-to-lysosome-associated degradation of proteasome-resistant ATZ polymers occurs via receptor-mediated vesicular transport. EMBO J 37, (2018).

25. Kamimoto T et al., Intracellular inclusions containing mutant alpha1-antitrypsin Z are propagated in the absence of autophagic activity. J Biol Chem 281, 4467–4476 (2006). [PubMed: 16365039]

26. Hidvegi T et al., An autophagy-enhancing drug promotes degradation of mutant alpha1-antitrypsin Z and reduces hepatic fibrosis. Science 329, 229–232 (2010). [PubMed: 20522742]

27. Kruse KB, Brodsky JL, McCracken AA, Characterization of an ERAD gene as VPS30/ATG6 reveals two alternative and functionally distinct protein quality control pathways: one for soluble Z variant of human alpha-1 proteinase inhibitor (A1PiZ) and another for aggregates of A1PiZ. Mol. Biol. Cell 17, 203–212 (2006). [PubMed: 16267277]

28. Travers KJ et al., Functional and genomic analyses reveal an essential coordination between the unfolded protein response and ER-associated degradation. Cell 101, 249–258 (2000). [PubMed: 10847680]

29. Cox JS, Shamu CE, Walter P, Transcriptional induction of genes encoding endoplasmic reticulum resident proteins requires a transmembrane protein kinase. Cell 73, 1197–1206 (1993). [PubMed: 8513503]

30. Yorimitsu T, Nair U, Yang Z, Klionsky DJ, Endoplasmic reticulum stress triggers autophagy. J Biol Chem 281, 30299–30304 (2006). [PubMed: 16901900]
31. Jin M et al., Transcriptional regulation by Pho23 modulates the frequency of autophagosome formation. Curr Biol 24, 1314–1322 (2014). [PubMed: 24881874]
32. Jeong YT et al., The ULK1-FBXW5-SEC23B nexus controls autophagy. eLife 7, (2018).
33. Grumati P et al., Full length RTN3 regulates turnover of tubular endoplasmic reticulum via selective autophagy. eLife 6, (2017).
34. Fumagalli F et al., Translocon component Sec62 acts in endoplasmic reticulum turnover during stress recovery. Nat. Cell Biol 18, 1173–1184 (2016). [PubMed: 27749824]
35. Chen Q et al., ATL3 Is a Tubular ER-Phagy Receptor for GABARAP-Mediated Selective Autophagy. Curr Biol 29, 846–855 e846 (2019). [PubMed: 30773365]
36. Chino H, Hatta T, Natsume T, Mizushima N, Intrinsically Disordered Protein TEX264 Mediates ER-phagy. Mol Cell, (2019).
37. An H et al., TEX264 Is an Endoplasmic Reticulum-Resident ATG8-Interacting Protein Critical for ER Remodeling during Nutrient Stress. Mol Cell, (2019).
38. Luo L et al., De-silencing Grb10 contributes to acute ER stress-induced steatosis in mouse liver. J Mol Endocrinol 60, 285–297 (2018). [PubMed: 29555819]
39. Liang JR, Lingeman E, Ahmed S, Corn JE, Atlastins remodel the endoplasmic reticulum for selective autophagy. J Cell Biol 217, 3354–3367 (2018). [PubMed: 30143524]
40. Wang S, Tukachinsky H, Romano FB, Rapoport TA, Cooperation of the ER-shaping proteins atlastin, lunapark, and reticulons to generate a tubular membrane network. eLife 5, (2016).
41. Fink JK, Hereditary spastic paraplegia: clinico-pathologic features and emerging molecular mechanisms. Acta Neuropathol 126, 307–328 (2013). [PubMed: 23897027]
42. Breuss MW et al., Mutations in LNPK, Encoding the Endoplasmic Reticulum Junction Stabilizer Lunapark, Cause a Recessive Neurodevelopmental Syndrome. Am J Hum Genet 103, 296–304 (2018). [PubMed: 30032983]
43. Wang B et al., The COPII cargo adapter SEC24C is essential for neuronal homeostasis. J Clin Invest 128, 3319–3332 (2018). [PubMed: 29939162]
44. Longtine MS et al., Additional modules for versatile and economical PCR-based gene deletion and modification in Saccharomyces cerevisiae. Yeast 14, 953–961 (1998). [PubMed: 9717241]
45. Lord C et al., Sequential interactions with Sec23 control the direction of vesicle traffic. Nature 473, 181–186 (2011). [PubMed: 21532587]
46. Bhandari D et al., Sit4p/PP6 regulates ER-to-Golgi traffic by controlling the dephosphorylation of COPII coat subunits. Mol. Biol. Cell 24, 2727–2738 (2013). [PubMed: 23864707]
47. Kanki T, Klionsky DJ, Mitophagy in yeast occurs through a selective mechanism. J Biol Chem 283, 32386–32393 (2008). [PubMed: 18818209]
48. Hutchins MU, Veenhuis M, Klionsky DJ, Peroxisome degradation in Saccharomyces cerevisiae is dependent on machinery of macroautophagy and the Cvt pathway. J Cell Sci 112 (Pt 22), 4079–4087 (1999). [PubMed: 10547367]
49. Griffith J, Mari M, De Maziere A, Reggiori F, A cryosectioning procedure for the ultrastructural analysis and the immunogold labelling of yeast Saccharomyces cerevisiae. Traffic 9, 1060–1072 (2008). [PubMed: 18429928]
50. Gelling CL, Dawes IW, Perlmutter DH, Fisher EA, Brodsky JL, The endosomal protein-sorting receptor sortilin has a role in trafficking alpha-1 antitrypsin. Genetics 192, 889–903 (2012). [PubMed: 22923381]
51. Hampton RY, Koning A, Wright R, Rine J, In vivo examination of membrane protein localization and degradation with green fluorescent protein. Proc Natl Acad Sci U S A 93, 828–833 (1996). [PubMed: 8570643]
52. Larson LL, Parrish ML, Koning AJ, Wright RL, Proliferation of the endoplasmic reticulum occurs normally in cells that lack a functional unfolded protein response. Yeast 19, 373–392 (2002). [PubMed: 11870859]

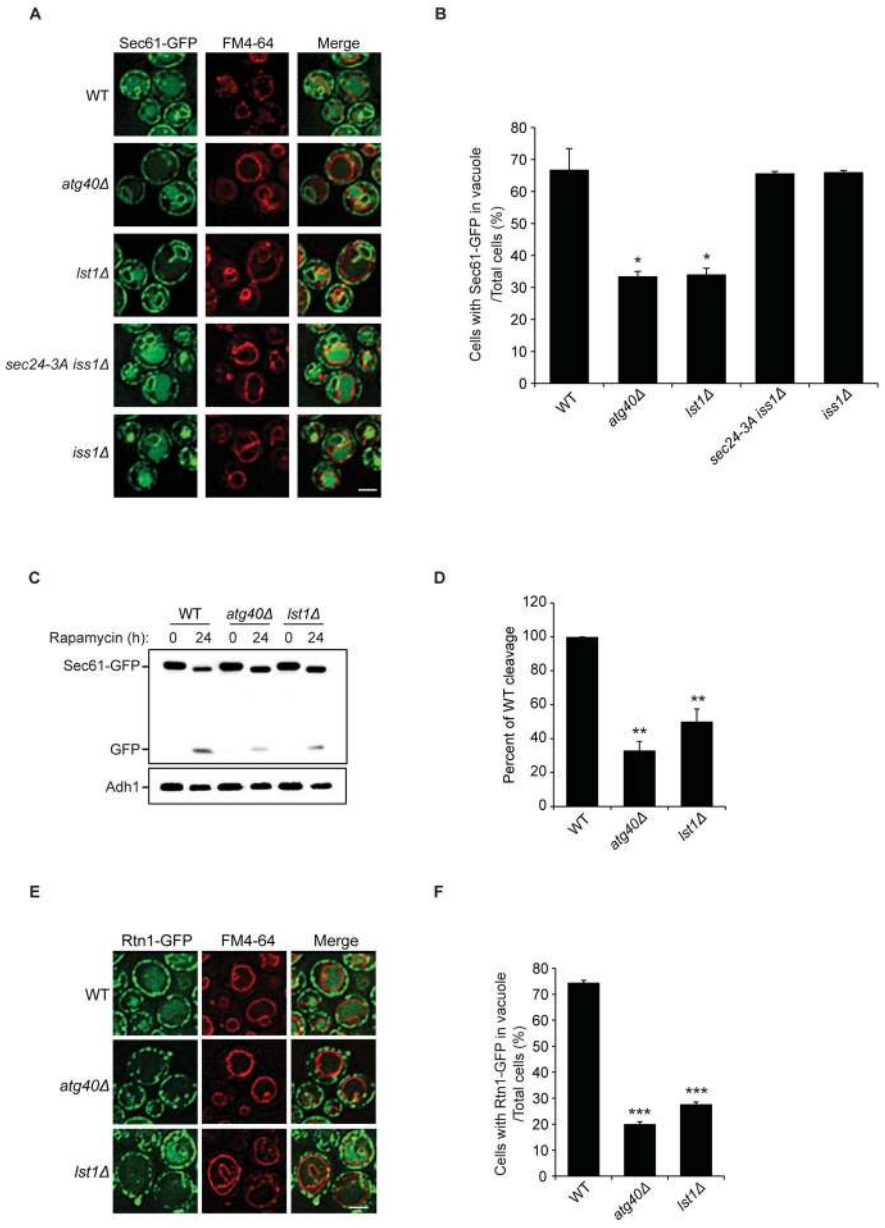

Figure 1. Lst1 is required for ER-phagy.

(**A**) The translocation of Sec61-GFP to the vacuole was examined by fluorescence microscopy in WT and mutant cells 24 h after rapamycin treatment. FM4-64 was used to stain the vacuolar membrane. (**B**) The percent of cells with Sec61-GFP delivered to the vacuole was quantitated from 300 cells. (**C**) The cleavage of Sec61-GFP to GFP in WT and mutant strains was analyzed by immunoblotting using anti-GFP antibody. A representative blot is shown. (**D**) Three separate experiments were used to quantitate the ratio of free GFP to Sec61-GFP from the data in (**C**). WT was set to 100%. (**E**) The translocation of Rtn1-GFP to the vacuole in WT and mutant cells was detected by fluorescence microscopy 24h after rapamycin treatment. (**F**) The percent of cells with Rtn1-GFP delivered to the vacuole

was quantitated from 300 cells. Scale bars in (**A**), (**E**), 5μm. Error bars in (**B**), (**D**), and (**F**) represent S.E.M., N=3; *P < 0.05, **P < 0.01, ***P < 0.001, Student's unpaired t-test.

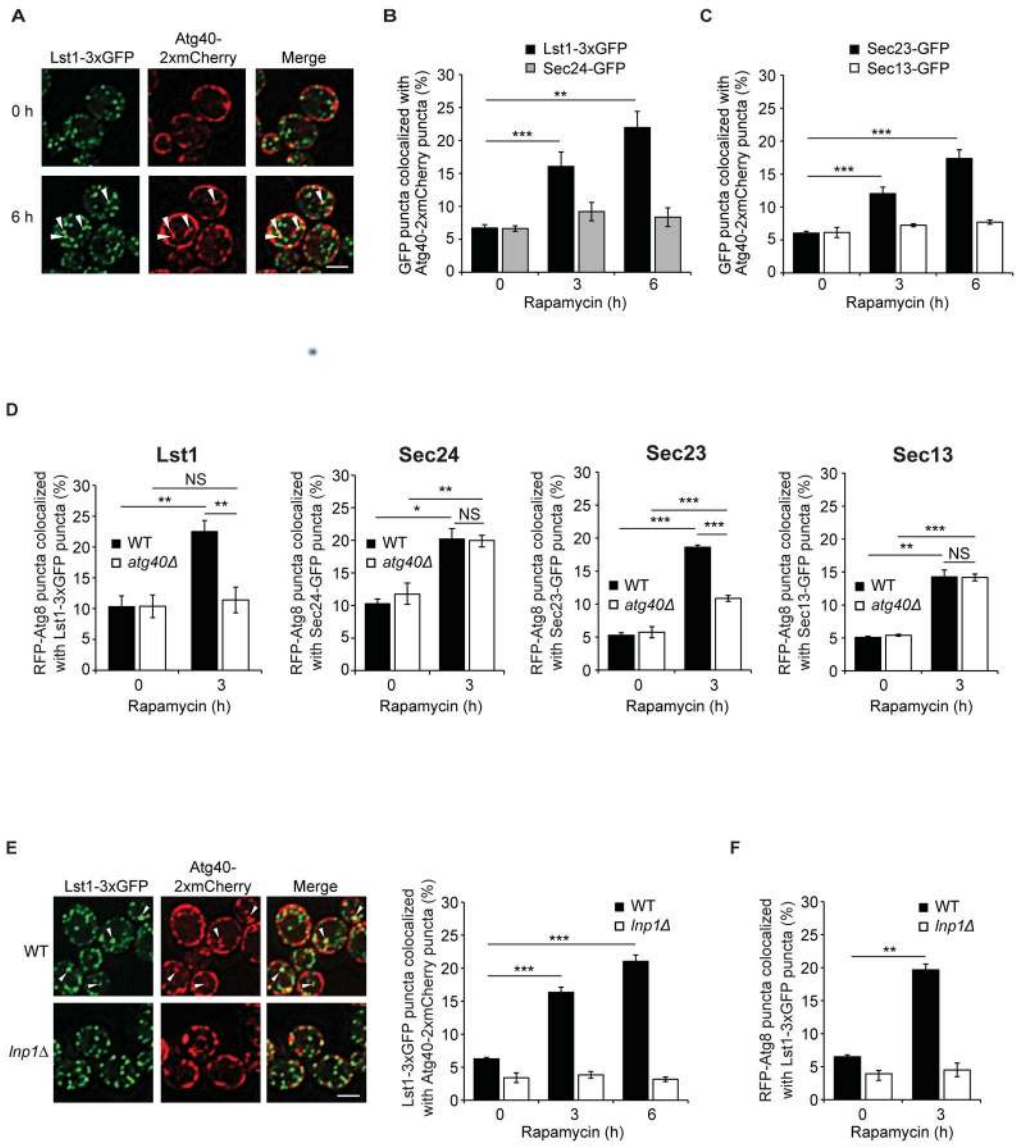

Figure 2. Lst1 and Sec23 colocalize with Atg40 and Atg8 in rapamycin-treated cells.

(**A**) Representative images of cells treated for 0 or 6 h with rapamycin. Arrowheads indicate Lst1-3xGFP that colocalize with Atg40-2xmCherry puncta. (**B**) Bar graph shows the percent of Lst1-3xGFP or Sec24-GFP colocalizing with Atg40-2xmCherry puncta. (**C**) Bar graph shows the percent of Sec23-GFP or Sec13-GFP colocalizing with Atg40-2xmCherry puncta. (**D**) Cells were treated for 0 or 3 h with rapamycin, and RFP-Atg8 that colocalizes with GFP tagged COPII coat subunits was quantitated. (**E**) Left, arrowheads indicate Lst1-3xGFP that colocalizes with Atg40-2xmCherry puncta 6 h after rapamycin treatment. Quantitation is on the right. (**F**) Quantitation of RFP-Atg8 that colocalize with Lst1-3xGFP in WT and *Inp1Δ* cells. Scale bars in (**A**), (**E**), 5μm. Error bars in (**B-F**) represent S.E.M., N=3-6; NS, not significant P ≥0.05, *P < 0.05, **P < 0.01, ***P < 0.001, Student's unpaired t-test.

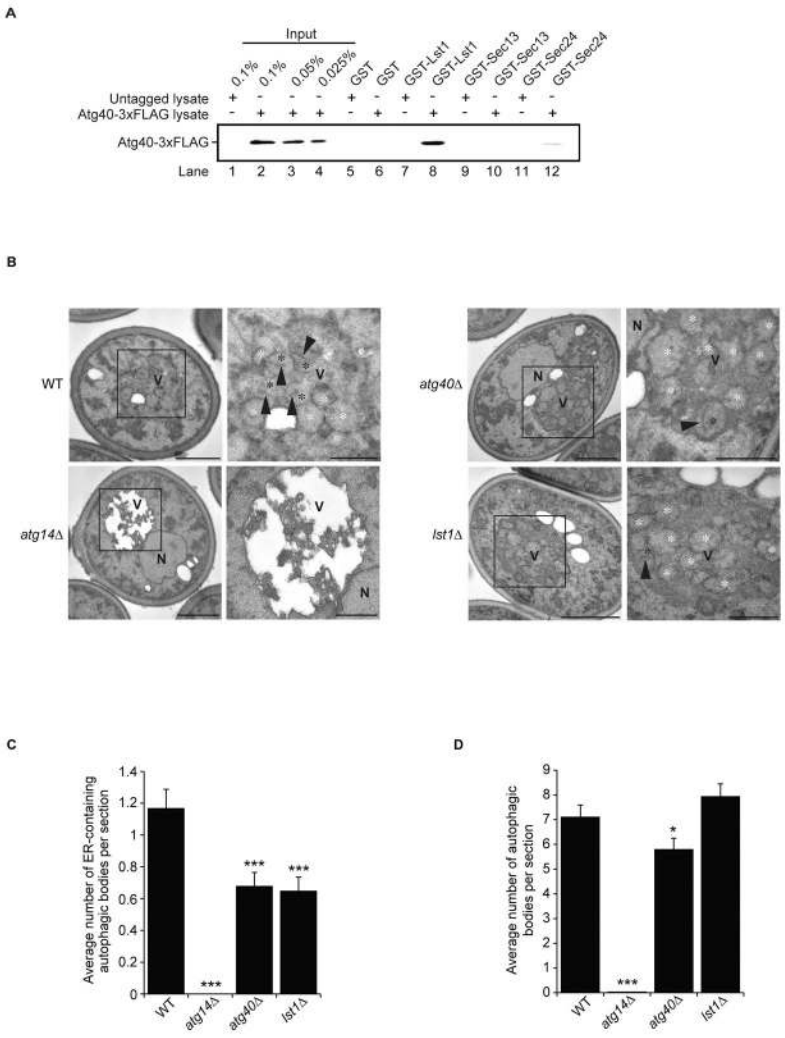

Figure 3. Lst1 binds to Atg40 and facilitates the packaging of ER into autophagosomes.

(**A**) Equimolar amounts (0.1 μM) of purified recombinant GST and GST fusion proteins were incubated with 2mg of yeast lysate prepared from Atg40-3xFLAG untagged or tagged cells treated with rapamycin. (**B**) Representative electron micrographs of WT and *pep4Δ* strains treated for 12 h with rapamycin. The boxed areas in the left panels are magnified on the right. Black asterisk, an autophagic body containing an ER fragment; white asterisk, an autophagic body lacking an ER fragment; arrowhead, an ER fragment inside an autophagic body. Scale bars in the left and right panels represent 1μm and 500 nm, respectively. (**C**) Bar graph showing the average number of ER-containing autophagosomes. (**D**) Bar graph showing the average number of total autophagosomes. Error bars in (**C**) and (**D**) represent S.E.M., N=100 cells; *P < 0.05, ***P < 0.001, Student's unpaired t-test. Symbols: N, nucleus; V, vacuole.

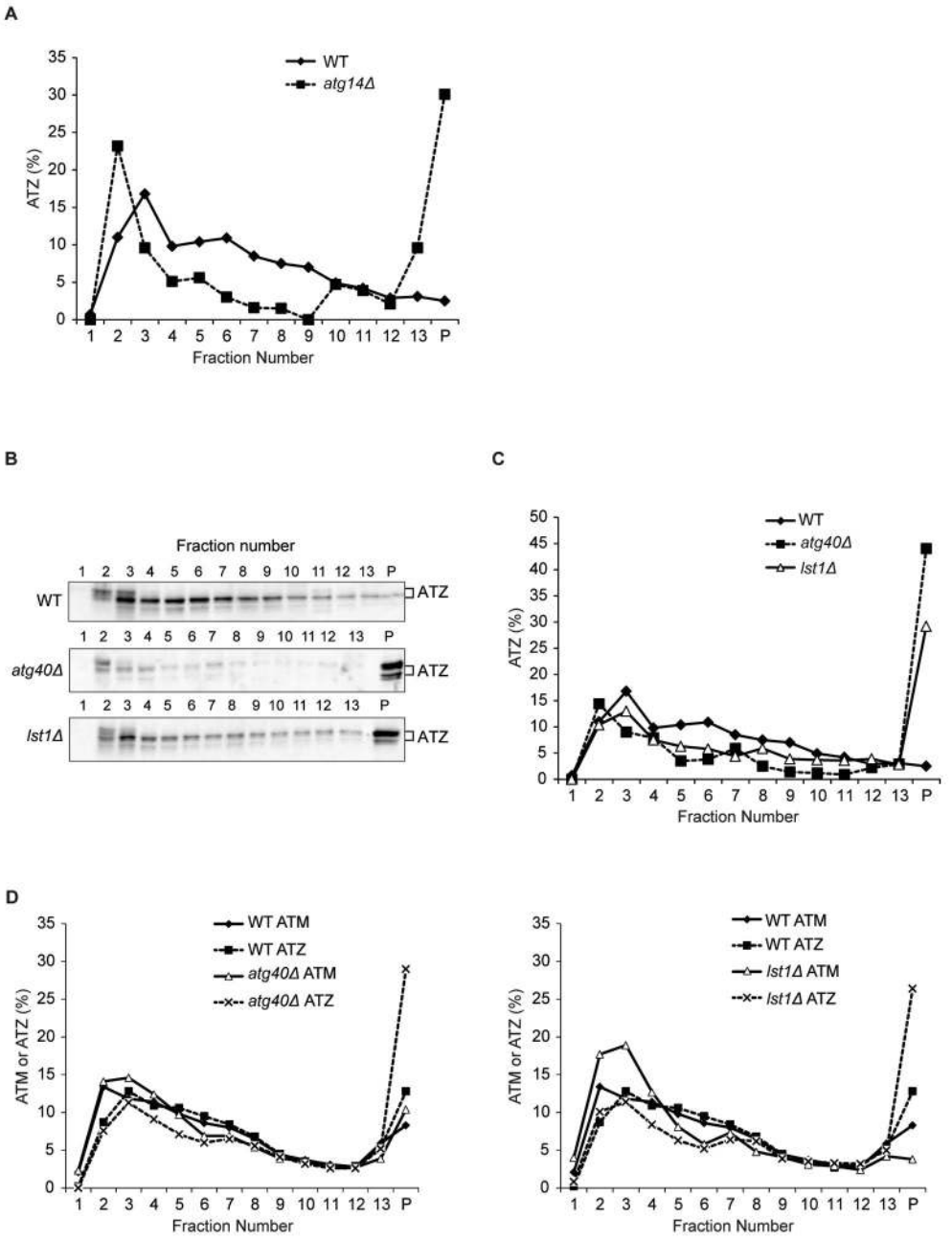

Figure 4. ATZ aggregates accumulate in *atg40*Δ and *lst1*Δ mutants.

Microsomal membrane fractions prepared from WT and mutant cells, harboring plasmids expressing either ATZ (**A-D**) or ATM (**D**), were lysed in the presence of detergent and fractionated on a sucrose gradient. Gradient fractions were blotted with antibody directed against alpha-1 antitrypsin. Soluble alpha-1 antitrypsin was at the top of the gradient and aggregates reside in the pellet (P).

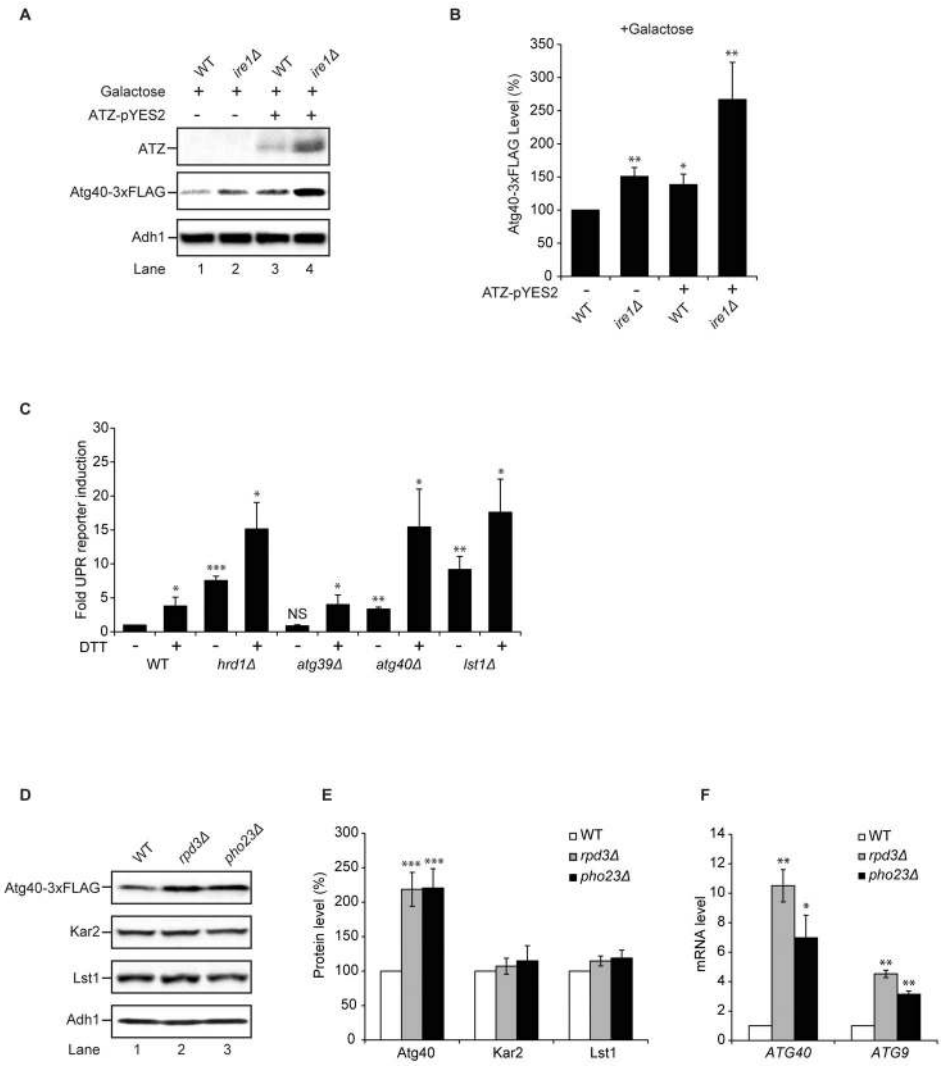

Figure 5. Atg40 expression is regulated by the Rpd3-Pho23 complex.

(**A**) Atg40 expression was examined 24 h after growth in 2% galactose. Western blot analysis was performed on lysates to detect ATZ (top), Atg40-3xFLAG (middle) and Adh1 (bottom). (**B**) The data in (**A**) were normalized to Adh1, and WT (-ATZ) was set to 100%. (**C**) UPR induction was assayed by flow cytometry in the absence or presence of 8mM DTT. WT (-DTT) was set to 1.0. (**D**) Atg40-3xFLAG, Kar2 and Lst1 levels were measured by western blot analysis in the indicated strains. (**E**) The data in (**D**) were normalized to Adh1 and WT was set to 100%. (**F**) qRT-PCR was used to assess mRNA levels. The data were normalized to actin mRNA levels, and WT was set to 1.0. Error bars in (**B**, **C,** and **F**) represent S.E.M., N=3. Error bars in (**E**) represent S.E.M., N=4-8. NS, not significant, $P \geq 0.05$, *$P < 0.05$, **$P < 0.01$, ***$P < 0.001$, Student's unpaired t-test.

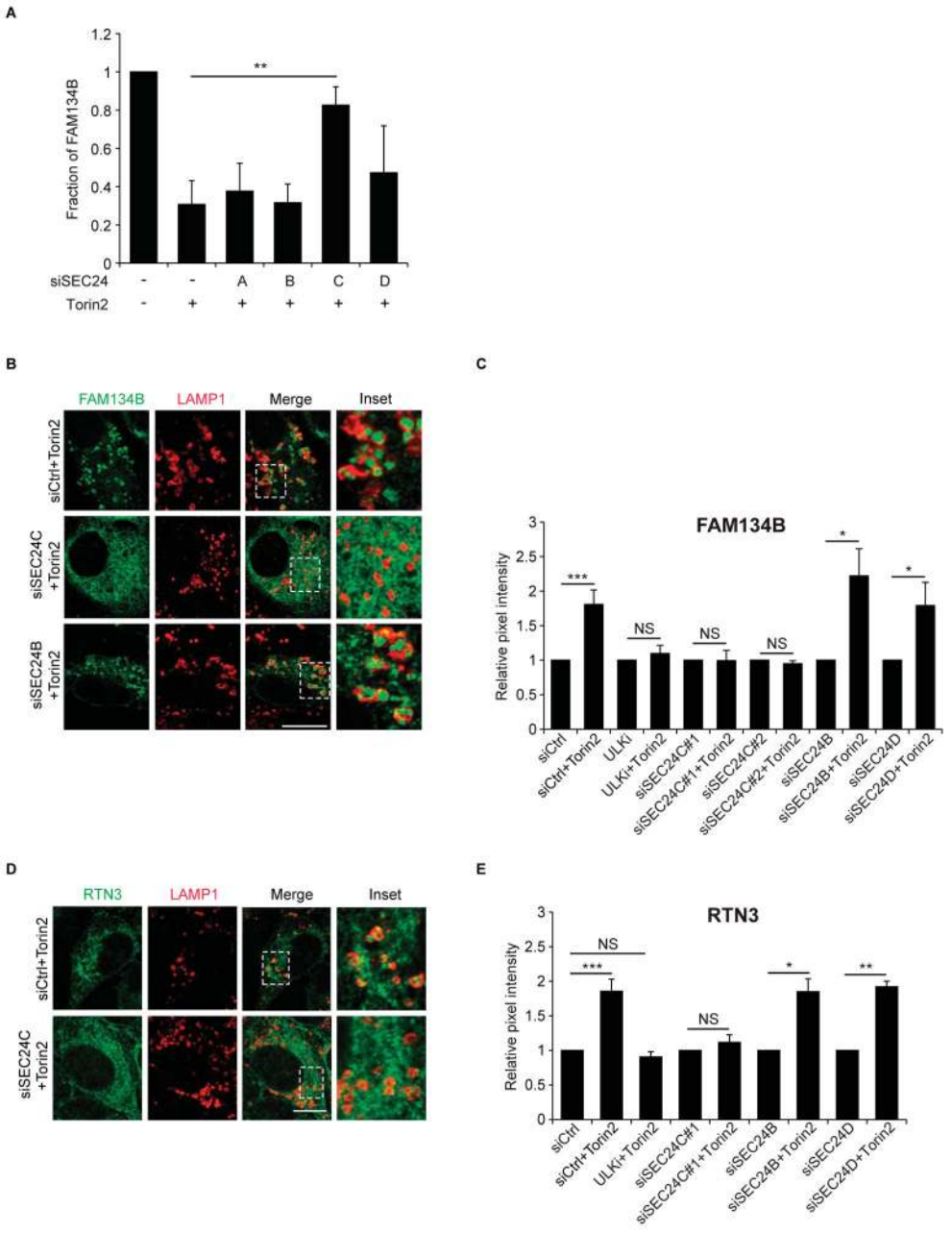

Figure 6. SEC24C is required for ER-phagy.

(**A**) Quantitation of 3xFLAG-FAM134B degradation from Torin2 treated control siRNA or SEC24 siRNA depleted U2OS cells normalized to actin. (**B and D**) Representative images of siRNA depleted cells treated with Torin2 and Bafilomycin A1. Quantitation of 3x-FLAG-FAM134B (**C**) or RTN3 (**E**) in LAMP1 structures. The DMSO control for each condition was set to 1.0. The data for two different siSEC24C duplexes is shown in **C**. Scale bar in (**B and D**) is 10μm. Error bars in (**A**, **C, E**) represent S.E.M., N=3-5, 50-70 cells/experiment for FAM134B (**C**) and 30 cells/experiment for RTN3 (**E**); NS, not significant P ≥0.05, *P < 0.05, **P < 0.01, ***P < 0.001, Student's unpaired t-test.